Mesoscopic effects in a single-mode Datta-Das spin field-effect transistor

Hyun-Woo Lee,* S. Çalışkan, and Hyowon Park
Department of Physics, Pohang University of Science and Technology, Pohang, Kyungbuk 790-784, Korea
(Received 10 August 2005; published 5 October 2005)

We study a single-mode Datta-Das spin field-effect transistor (SFET) in the presence (absence) of impurity scattering and external magnetic fields, and find interesting mesoscopic effects such as peak splitting, phase locking, and period halving. Experimental observation of these effects appears to be feasible in a single-mode SFET made of materials such as InGaAs/InAlAs.

DOI: 10.1103/PhysRevB.72.153305 PACS number(s): 73.63.−b, 72.25.−b

The spintronics[1] aims to utilize the spin of electrons. One of the representative spintronic systems is the Datta-Das spin field-effect transistor (SFET),[2,3] which utilizes the phase difference between spin-up and -down electrons caused by the Rashba spin-orbit interaction[4,5] in a two-dimensional electron gas (2DEG). Despite the intense experimental efforts, the SFET has not yet been realized.[3] There are theoretical indications that the spin relaxation is severely suppressed in a quasi-one-dimensional SFET (Ref. 6) even when it is not strictly ballistic. Moreover it is suggested that to achieve a SFET with large current modulation and low power consumption, which is one of the prime advantages of spintronics over conventional electronics, a SFET with only one transverse mode is desired.[7]

In this paper, we report interesting mesoscopic effects in a single-mode SFET [Fig. 1(a)], where a 2DEG of length L is connected to a spin-selective injector and collector, both of which are assumed to be magnetized along the x-direction and ideal.[8] With y-axis as its growth direction, the 2DEG in the xz-plane is described by

$$H_{2D}=\frac{p_x^2+p_z^2}{2m^*}+V_c(z)+\frac{\alpha}{\hbar}(\sigma_z p_x-\sigma_x p_z)+V_{sc}(x,z), \quad (1)$$

where the transverse confinement potential $V_c(z)$ is 0 for $|z|<w/2$ and ∞ for $|z|>w/2$, and w is smaller than $\sqrt{2\pi/n_s}$, n_s being the electron density in the 2DEG, so that only one transverse mode is allowed.[9] Here σ_x and σ_z are the Pauli matrices, $V_{sc}(x,z)$ is a nonmagnetic scattering potential, m^* is the effective mass, and α is the Rashba spin-orbit interaction parameter. For various candidate systems of the SFET such as InGaAs/InAlAs,[5] InAs/GaSb,[10] InAs/AlSb,[11] and CdTe/HgTe/CdTe,[12] the dimensionless number $(m^*\alpha/\hbar^2)\sqrt{2\pi/n_s}$ ranges from 0.01 to 0.1. Combined with the single-mode constraint $w<\sqrt{2\pi/n_s}$, we assume below $m^*\alpha w/\hbar^2\ll 1$, implying negligible spin variation along the transverse direction.

When $m^*\alpha w/\hbar^2\ll 1$, a ballistic $[V_{sc}(x,z)=0]$ single-mode SFET can be described by an effective one-dimensional (1D) Hamiltonian,[2] $H_{1D}^{\text{ballistic}}=p_x^2/2m^*+\alpha\sigma_z p_x/\hbar+E_{tr}-m^*\alpha^2/2\hbar^2$, which produces an exact energy dispersion relation of H_{2D} [Fig. 1(b)] up to the second order in $m^*\alpha w/\hbar^2$. Here $E_{tr}\equiv\pi^2\hbar^2/2m^*w^2$ arises from the transverse quantization and the last term is a correction to E_{tr} due to $-\alpha\sigma_x p_z/\hbar$ in H_{2D}.

The application of the Landauer formula[9] to a SFET results in the zero temperature ($T=0$) two-terminal conductance,

$$G=\frac{e^2}{h}\frac{4\cos^2\frac{\phi_0}{2}\sin^2\bar{k}L}{\sin^4\frac{\phi_0}{2}+4\cos^2\frac{\phi_0}{2}\sin^2\bar{k}L}, \quad (2)$$

where $\phi_0\equiv 2m^*\alpha L/\hbar^2$ is the spin precession angle over length L, $\bar{k}\equiv(k_\uparrow^F+k_\downarrow^F+k_\uparrow^B+k_\downarrow^B)/4$ is the average Fermi wave vector, and $k_{\uparrow(\downarrow)}^F$ and $-k_{\uparrow(\downarrow)}^B$ are, respectively, the Fermi wave vectors for forward and backward motion of spin up $\sigma_z=1$ (spin down $\sigma_z=-1$) electrons at the Fermi energy E_F [Fig. 1(b)]. Note that Eq. (2) differs from the conventional expression $G=(e^2/h)\cos^2(\phi_0/2)$. Physically this difference arises from the interference of the Fabry-Perot-like multiple reflection trajectories between the injector and collector [see Fig. 2(a)], which has been previously discussed in Ref. 13. According to Eq. (2), the conductance peak width varies considerably with E_F since $\bar{k}L\approx m^*v_FL/\hbar+(m^*\alpha L/\hbar^2)(\alpha/\hbar v_F)$ changes by π when E_F changes by $\pi\hbar v_F/L$. Here v_F is the Fermi velocity and $\alpha/(\hbar v_F)$ $[\sim(m^*\alpha/\hbar^2)\sqrt{2\pi/n_s}\ll 1]$ is assumed to be small. At finite temperatures, the E_F-dependence is weakened by the thermal averaging and disappears for $k_BT\gg\pi\hbar v_F/L$; $G=(2e^2/h)\cos^2(\phi_0/2)/[1+\cos^2(\phi_0/2)]$, which still differs from the conventional result. Equation (2) is found to be in good agreement with the results [Fig. 3(a)] of our numerical calculation for the original 2D Hamiltonian H_{2D} via the tight-binding (TB) approximation[14] that takes into account not only the 2DEG but also the injector and collector.[15]

Mesoscopic effects become more pronounced when an external magnetic field $\vec{B}_{ext}=B_\parallel\hat{z}$ is applied parallel to the effective magnetic field due to the Rashba interaction. Below we assume $g^*\mu_BB_\parallel\ll E_F-E_{tr}$, where g^* is the effective gyro-

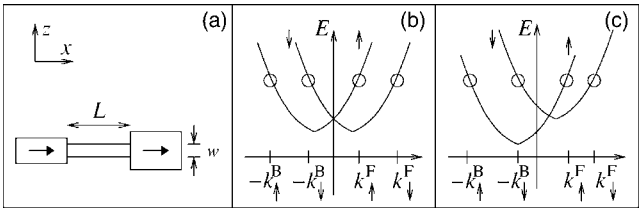

FIG. 1. The schematic drawing of a Datta-Das spin field-effect transistor (a), the energy dispersion relations without magnetic field (b), and with magnetic field $B_\parallel$ parallel to $\hat{z}$ (c).

 ©2005 The American Physical Society

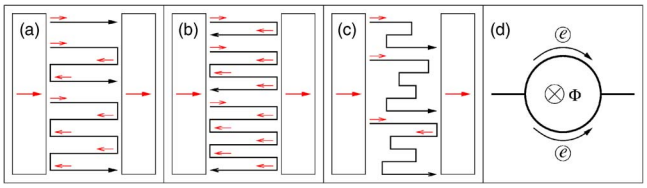

FIG. 2. (Color online) Electron trajectories contributing to the transmission probability in a ballistic system (a), and trajectories contributing to the reflection probability in a ballistic system (b). In a nonballistic system, additional trajectories contribute to the transmission (c). Small (red) arrows in (a,b,c) indicate the spin direction right after the injection or right after the reflection. (d) The schematic drawing of an Aharonov–Bohm interferometer with a threading magnetic flux Φ.

magnetic ratio and μ_B is the Bohr magneton. With the effective Hamiltonian $H_{1D}^{\text{ballistic},B_\parallel} \equiv H_{1D}^{\text{ballistic}} - g^* \mu_B B_\parallel \sigma_z$, the energy dispersion relation is modified as shown in Fig. 1(c). The conventional approximation, which takes into account only the first trajectory in Fig. 2(a), results in $G = (e^2/h)\cos^2[(\phi_0 - \delta\phi)/2]$, where $\delta\phi \equiv 2g^*\mu_B B_\parallel/(\hbar v_F/L)$ represents the spin precession by $B_\parallel$. Thus all conductance peaks are predicted to shift by $\delta\alpha \equiv \delta\phi/(2m^*L/\hbar^2) = g^*\mu_B B_\parallel \hbar/m^* v_F$. On the other hand, correct summation of all trajectories in Fig. 2(a) results in

$$\frac{G}{e^2/h} = \frac{4\left(\cos^2\frac{\phi_0}{2} - \sin^2\frac{\delta\phi}{2}\right)\sin^2 \bar{k}L + 4\sin^2\frac{\phi_0}{2}\sin^2\frac{\delta\phi}{2}}{\left(\sin^2\frac{\phi_0}{2} + \sin^2\frac{\delta\phi}{2}\right)^2 + 4\left(\cos^2\frac{\phi_0}{2} - \sin^2\frac{\delta\phi}{2}\right)\sin^2 \bar{k}L}, \tag{3}$$

which predicts that upon the application of $B_\parallel$, each peak *splits* into two, one drifting to the left and the other drifting to the right by the amount $|\delta\alpha|$. The numerical calculation result [Fig. 3(b)] for $H_{2D}^{B_\parallel} \equiv H_{2D} - g^*\mu_B B_\parallel \sigma_z$ is in good agreement with the prediction of Eq. (3). Physically the peak splitting arises from the difference between $(k_\downarrow^F - k_\uparrow^F)L = \phi_0 - \delta\phi$ and $(k_\uparrow^B - k_\downarrow^B)L = \phi_0 + \delta\phi$ [Fig. 1(c)], which represent the total spin precession angles (due to α and $B_\parallel$)

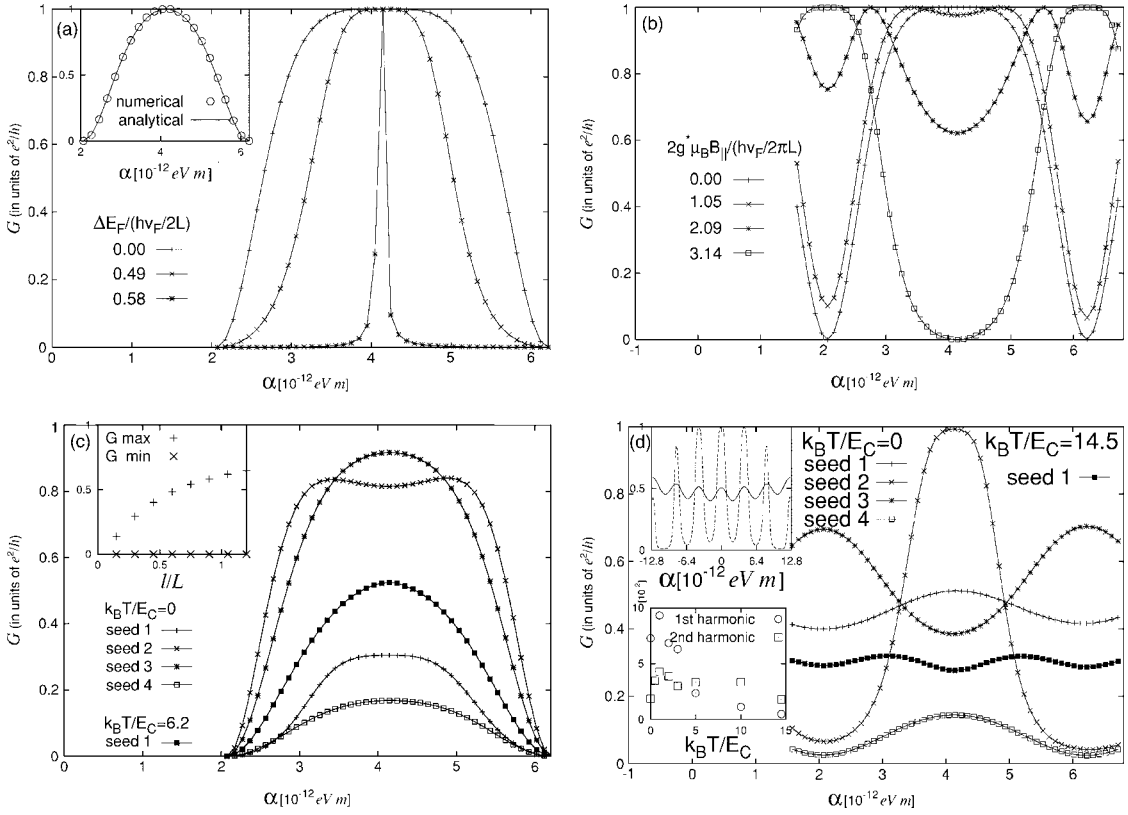

FIG. 3. Conductance G of a SFET that consists of a 2DEG, ideal injector, and collector (Ref. 15). $H_{2D}^{B_\parallel}$ is approximated by a 2D tight-binding Hamiltonian.[14] The following parameters are used: $m^* = 0.04\, m_{\text{electron}}$, $n_s = 1.7 \times 10^{12}$ cm^{-2}, $g^*\mu_B = 1.3 \times 10^{-23}$ J/T, $w = 0.7 \times (2\pi/n_s)^{1/2} (\ll \hbar^2/m^*\alpha)$, and $L = 1.44$ μm, where m_{electron} is the free electron mass. (a) The ballistic case with $B_\parallel = 0$: The variation of $G(\alpha)$ with E_F at $T = 0$. Inset: $G(\alpha)$ at $k_BT = 10\hbar v_F/L$. The numerical result is in excellent agreement with the analytic high temperature expression $G = (2e^2/h)\cos^2(\phi_0/2)/[1 + \cos^2(\phi_0/2)]$. (b) The ballistic case with $B_\parallel \neq 0$: The variation of $G(\alpha)$ with $2g^*\mu_B B_\parallel/(\hbar v_F/L)$ at $T = 0$. (c) The nonballistic case with $B_\parallel = 0$: $G(\alpha)$ at $k_BT = 0$ and $k_BT = 6.2E_c$. The seed number represents different impurity configurations, all of which have the same ratio $l/L = 0.7$. The graph for the seed 3 shows the scattering-induced peak splitting. The mean free path l is evaluated by the first order Born approximation. Inset: Maximum and minimum values of $G(\alpha)$ as a function of l/L for the seed 1 at $k_BT = 6.2E_c$. (d) The nonballistic case with $2g^*\mu_B B_\parallel = 8\pi\hbar v_F/L = 8.7E_c$: $G(\alpha)$ at $k_BT = 0$ and $k_BT = 14.5E_c$. The seed number represents different impurity configurations, all of which still have the same ratio $l/L = 0.3$. Note the period halving. Upper inset: $G(\alpha)$ at $l/L = 0.3$ (solid line for seed 1, dashed line for seed 2) and $T = 0$. The symmetry $G(\alpha) = G(-\alpha)$ holds for general $B_\parallel$. Lower inset: Magnitudes of the first (with period $2\pi\hbar^2/2m^*L$) and second (with period $\pi\hbar^2/2m^*L$) harmonic components of $G(\alpha)$ for $l/L = 0.3$ (seed 1) as a function of the scaled temperature k_BT/E_c.

for forward and backward motion, respectively. Interestingly $\cos^2[(\phi-\delta\phi)/2]=1$ for the right-drifting peaks and $\cos^2[(\phi+\delta\phi)/2]=1$ for the left-drifting peaks ($B_\parallel>0$ assumed). In the latter peaks, each trajectory for the reflection probability of the forward moving electrons [Fig. 2(b)] gives a vanishing contribution. The peak splitting persists up to considerably high temperature $k_BT\sim[(E_F-E_{\rm tr})/g\mu_BB_\parallel](\pi\hbar v_F/L)$ since E_F-variation by this energy scale does not alter $\delta\alpha$ significantly.

In a nonballistic case [$V_{\rm sc}(x,z)\neq 0$], the reduction of $H^{B_\parallel}_{\rm 2D}$ to an effective 1D Hamiltonian is less trivial since $V_{\rm sc}(x,z)$ is known to cause not only spin-conserving scattering but also *spin-flipping* scattering (spin$\uparrow\leftrightarrow$spin$\downarrow$) via the Elliot–Yafet (EY) mechanism.[16] The spin-flipping scattering rate can be estimated as follows: In the first order Born approximation, the spin flipping rate from spin s to $-s$ is proportional to $|\langle\psi_{-s}(k')|V_{\rm sc}|\psi_s(k)\rangle|^2$, where the energy eigenstate $|\psi_s(k)\rangle$ in the absence of $V_{\rm sc}$ is given in Ref. 17 by $e^{ikx}\varphi_0(z)[\cos(m^*\alpha z/\hbar^2)|s\rangle+i\sin(m^*\alpha z/\hbar^2)|-s\rangle+\mathcal{O}(m^*\alpha w/\hbar^2)^2]$ and $\varphi_0(z)$ is the transverse wave function of the lowest mode. Note that the nominal spin s state $|\psi_s(k)\rangle$ contains not only the spin s but also $-s$ component due to the Rashba interaction and thus has spin texture along the z-axis.[18] A straightforward calculation shows that the spin flipping rate is proportional to $|\mathcal{O}(m^*\alpha w/\hbar^2)^2|^2=\mathcal{O}(m^*\alpha w/\hbar^2)^4\ll 1$. Thus the spin-flipping scattering can be safely neglected and one obtains $H^{B_\parallel}_{\rm 1D}=p_x^2/2m^*+\alpha\sigma_zp_x/\hbar+V_\alpha(x)+E_{\rm tr}-m^*\alpha^2/2\hbar^2-g^*\mu_BB_\parallel\sigma_z$, where $V_\alpha(x)$ is an effective nonmagnetic scattering potential that in principle depends on α. The α-dependence is however found to be negligible when $m^*\alpha w/\hbar^2\ll 1$.

For $H^{B_\parallel}_{\rm 1D}$, G at $T=0$ becomes $G=(e^2/h)|F|^2$, where

$$F=2\frac{\hat t^{\rm F}_\uparrow\hat t^{\rm F}_\downarrow(\hat t^{\rm B}_\uparrow+\hat t^{\rm B}_\downarrow)-\hat t^{\rm F}_\uparrow(1-r^{\rm F}_\downarrow)(1-r^{\rm B}_\downarrow)-\hat t^{\rm F}_\downarrow(1-r^{\rm F}_\uparrow)(1-r^{\rm B}_\uparrow)}{(\hat t^{\rm F}_\uparrow+\hat t^{\rm F}_\downarrow)(\hat t^{\rm B}_\uparrow+\hat t^{\rm B}_\downarrow)-(2-r^{\rm F}_\uparrow-r^{\rm F}_\downarrow)(2-r^{\rm B}_\uparrow-r^{\rm B}_\downarrow)} \tag{4}$$

takes into account all possible nonballistic trajectories [Fig. 2(c)] as well. Here $\hat t^{\rm F/B}_{\uparrow(\downarrow)}\equiv\exp[ik^{\rm F/B}_{\uparrow(\downarrow)}L]t^{\rm F/B}_{\uparrow(\downarrow)}$, and $t^{\rm F/B}_{\uparrow(\downarrow)}$, and $r^{\rm F/B}_{\uparrow(\downarrow)}$ are respectively the transmission and reflection amplitudes of spin up (down) electrons incident from left (right).[19] Interestingly Eq. (4) is identical to the result [Eq. (3) in Ref. 20] for an Aharonov–Bohm interferometer [Fig. 2(d)], which exhibits various mesoscopic phenomena. This agreement is not a mere coincidence and a formally exact correspondence can be established; the spin up and down channels in a SFET vs. the upper and lower arms of an AB interferometer, and the spin-selective injector and collector of a SFET vs. the three-way splitters of an AB interferometer [Eq. (2) in Ref. 20]. Moreover α in a SFET corresponds to the threading magnetic flux Φ in an AB interferometer in the sense that they both induce the phase difference between two channels (arms). This relation between the two systems suggests that a SFET may show similar mesoscopic behaviors as an AB interferometer.

There is, however, a delicate difference between the two systems: While scattering amplitudes of the two arms in an AB interferometer are statistically independent, scattering amplitudes of the two spin channels in a SFET are correlated. To reveal the correlations, we use the gauge transformation $\tilde\Psi=\exp[i(m^*\alpha x/\hbar^2)\sigma_z]\Psi$, which maps $H^{B_\parallel}_{\rm 1D}$ to $\tilde H^{B_\parallel}_{\rm 1D}\equiv p_x^2/2m^*+V_\alpha(x)+E_{\rm tr}-m^*\alpha^2/\hbar^2-g^*\mu_BB_\parallel\sigma_z$. For $B_\parallel=0$, scattering amplitudes of $\tilde H^{B_\parallel=0}_{\rm 1D}$ satisfy $\tilde t^{\rm F/B}_\uparrow(E)=\tilde t^{\rm F/B}_\downarrow(E)$ $[\equiv\tilde t^{\rm F/B}_0(E)]$ and $\tilde r^{\rm F/B}_\uparrow(E)=\tilde r^{\rm F/B}_\downarrow(E)$ $[\equiv\tilde r^{\rm F/B}_0(E)]$ since spin is decoupled from orbital motion. Moreover $\tilde t^{\rm F}_0(E)=\tilde t^{\rm B}_0(E)$ $[\equiv\tilde t_0(E)]$ due to the time-reversal symmetry. Taking into account the Zeeman energy and the gauge transformation, one then obtains for $H^{B_\parallel}_{\rm 1D}$ the inter-channel correlations, $t^{\rm F/B}_\uparrow(E-g^*\mu_BB_\parallel)=t^{\rm F/B}_\downarrow(E+g^*\mu_BB_\parallel)$ $[=\tilde t_0(E)]$ and $r^{\rm F/B}_\uparrow(E-g^*\mu_BB_\parallel)=r^{\rm F/B}_\downarrow(E+g^*\mu_BB_\parallel)$ $[=\tilde r^{\rm F/B}_0(E)]$. When these inter-channel correlations are combined with the energy correlation within each channel, namely $\tilde t_0(E)$ [also $\tilde r^{\rm F/B}(E)$] as a function E being correlated over the Thouless correlation energy $E_{\rm c}\equiv\pi^2(\hbar v_F/L)(l/L)$,[21,22] where l is the mean free path, the scattering amplitudes of the spin-up and down channels at an *equal* energy are correlated if $2g^*\mu_BB_\parallel\ll E_{\rm c}$. In contrast, the two interfering arms in an AB interferometer do not have such correlations.

We first study the high field regime $2g^*\mu_BB_\parallel\gg E_{\rm c}$, where the inter-channel equal-energy correlations are negligible. To illustrate *scattering-induced* mesoscopic effects, it is useful to confine ourselves to special $B_\parallel$'s with $\sin\delta\phi=0$, where, in a ballistic case, left- and right-drifting peaks cross each other [see Fig. 3(b)] and even the conventional approximation predicts the peak positions correctly. For those $B_\parallel$'s and at $T=0$, the conventional approximation applied to a nonballistic case results in $G=(e^2/2h)\{(|t^{\rm F}_\uparrow|^2+|t^{\rm F}_\downarrow|^2)/2+|t^{\rm F}_\downarrow t^{\rm F}_\uparrow|\cos[\phi_0-\delta\phi+\arg(t^{\rm F}_\downarrow)-\arg(t^{\rm F}_\uparrow)]\}$, where $\arg(t^{\rm F}_{\uparrow/\downarrow})$ represents the phase of $t^{\rm F}_{\uparrow/\downarrow}$. Since $t^{\rm F}_\uparrow$ and $t^{\rm F}_\downarrow$ are independent of each other, the conventional approximation predicts a scattering-induced peak shift $\Delta\alpha=(\hbar^2/2m^*L)[\arg(t^{\rm F}_\downarrow)-\arg(t^{\rm F}_\uparrow)]$, which can have any value in principle. According to Eq. (4), however, $\Delta\alpha$ is *locked* to special values $(\hbar^2/2m^*L)n_{\rm locking}\pi$ [Fig. 3(d)], where $n_{\rm locking}$ is an integer. Roughly speaking $n_{\rm locking}$ is an integer nearest to $[\arg(t^{\rm F}_\downarrow)-\arg(t^{\rm F}_\uparrow)]/\pi$. This phase locking in a SFET is in correspondence with the phase locking in an AB interferometer.[23,24] The physical origin of the phase locking is a bit different in the two systems though. While the phase locking in an AB interferometer arises from the time-reversal symmetry, which enforces $G(\Phi)=G(-\Phi)$,[23] the phase locking in a SFET arises from *two* symmetries: the first symmetry being the time-reversal symmetry, which enforces $G(\alpha,B_\parallel,M_L,M_R)=G(\alpha,-B_\parallel,-M_L,-M_R)$ where $M_{L/R}$ is the magnetization of the injector (collector) along the x-axis, and the second symmetry being the spin rotation of the entire system by π about the y-axis followed by the simultaneous reversal of the magnetization, magnetic field, and α, which enforces $G(\alpha,B_\parallel,M_L,M_R)=G(-\alpha,-B_\parallel,-M_L,-M_R)$. The numerical calculation results of $H^{B_\parallel}_{\rm 2D}$ confirm the relation $G(\alpha,B_\parallel,M_L,M_R)=G(-\alpha,B_\parallel,M_L,M_R)$ [upper inset in Fig. 3(d)], which is a combined result of the two symmetries. The numerical results [Fig. 3(d)] are also in good agreement with the phase locking prediction. Note that $n_{\rm locking}$ and also the oscillation amplitude fluctuate considerably among different realizations of $V_\alpha(x)$, all of which still have the same ratio l/L. These fluctuations are due to the well known phenomenon of conductance fluctuations.[9]

The E_F-dependent fluctuations of scattering amplitudes implies that the integer n_{locking} also fluctuates with E_F and is correlated over the energy scale E_c. Thus at high temperatures ($k_BT \gg E_c$), the energy dependent fluctuation of n_{locking} is expected to self-average and suppress the conductance oscillation with α. The way the oscillation is suppressed is rather peculiar however. As shown in the lower inset of Fig. 3(d), the self-averaging suppresses only the first harmonic component of the α-dependent oscillation (with period $2\pi\hbar^2/2m^*L$) while the second harmonic component (with period $\pi\hbar^2/2m^*L$) is not significantly affected. As a result, the oscillation period at high temperatures is reduced to half of the original value [Fig. 3(d)], which is in an exact correspondence with the period halving in an AB interferometer (Ref. 25) due to the temperature-induced self-averaging. We also remark that the suppression of the first harmonic component is not specific to the special $B_\parallel$'s used for illustration but occurs for arbitrary $B_\parallel$ with $2g^*\mu_B B_\parallel \gg E_c$.

Next we study the low field regime $2g^*\mu_B B_\parallel \ll E_c$. In particular, we focus on the zero field case, where perfect equal-energy correlations exist between the two spin channels: $t_\uparrow^{F/B}(E) = t_\downarrow^{F/B}(E)$ [$=\tilde{t}_0(E)$], and $r_\uparrow^{F/B}(E) = r_\downarrow^{F/B}(E)$ [$=\tilde{r}_0^{F/B}(E)$]. An immediate consequence is the identically vanishing conductance for $\cos^2(\phi_0/2)=0$, which uniquely fixes the integer n_{locking} to be zero. The correlations also prevent the period halving at high temperatures since n_{locking} does not fluctuate with E_F. Then the magnitude of the first harmonic component can be estimated by the conductance at $\cos^2(\phi_0/2)=1$, which is $G=(e^2/h)|\tilde{t}_0(E_F)|^2$ at $T=0$. We remark that the oscillation amplitude suppression of G by the factor $|\tilde{t}_0(E_F)|^2$ is not due to the spin relaxation but rather due to the imperfect transmission probability $|\tilde{t}_0(E_F)|^2$, which fluctuates from sample to sample by order 1 due to the phenomenon of the conductance fluctuations.[9] We also remark that occasionally the magnitude of the second harmonics is comparable to the magnitude of the harmonics, which may result in a *scattering-induced* peak splitting. At high temperatures $k_BT \gg E_c$, the peak splitting disappears due to the thermal averaging of E-dependent fluctuations and the peak conductance at $\cos^2(\phi_0/2)=1$ is roughly given by $(e^2/h)(l/L)$ for $l/L \lesssim 1$.[26] These predictions are in good agreement with the numerical calculation results of H_{2D} in Fig. 3(c).

We remark that the predicted mesoscopic effects can be revealed only when both spin and orbital degrees of freedom are analyzed quantum mechanically and thus go beyond semiclassical treatments (Ref. 6) that ignore quantum mechanical nature of the orbital degree of freedom. We also remark that our preliminary numerical calculation for *three* transverse modes also shows peak splitting, phase locking, and period halving. Thus the predicted mesoscopic effects are not restricted to a single-mode SFET only. Further studies on a SFET with multiple transverse modes are necessary. Finally we expect that the predicted mesoscopic effects can be observed in a single-mode SFET made of materials such as InGaAs/InAlAs,[5] InAs/GaSb,[10] InAs/AlSb,[11] and CdTe/HgTe/CdTe,[12] for which our assumption $m^*\alpha w/\hbar^2 \ll 1$ holds.

We acknowledge H.-S. Sim and J.-S. Jeong for their help on numerical calculations. The authors were supported by SRC/ERC program (Grant No. R11–2000–071) and the Basic Research Program (Grant No. R01-2005-000-10352-0) of MOST/KOSEF.

*Electronic address: hwl@postech.ac.kr

[1] G. A. Prinz, Phys. Today **48**, 58 (1995); Science **282**, 1660 (1998); S. A. Wolf *et al.*, Science **294**, 1488 (2001).
[2] S. Datta and B. Das, Appl. Phys. Lett. **56**, 665 (1990).
[3] For a recent review, see for instance, I. Zutic *et al.*, Rev. Mod. Phys. **76**, 323 (2004).
[4] Yu. A. Bychkov and E. I. Rashba, J. Phys. C **17**, 6039 (1984); JETP Lett. **39**, 78 (1984).
[5] J. Nitta *et al.*, Phys. Rev. Lett. **78**, 1335 (1997).
[6] A. Bournel *et al.*, Solid State Commun. **104**, 85 (1997); A. Bournel *et al.*, Eur. Phys. J.: Appl. Phys. **4**, 1 (1998); A. A. Kiselev and K. W. Kim, Phys. Rev. B **61**, 13115 (2000).
[7] E. Shafir *et al.*, Phys. Rev. B **70**, 241302(R) (2004); S. Pramanik *et al.*, IEEE Trans. Nanotechnol. **4**, 2 (2005).
[8] Both injector and collector are assumed to be 100% spin polarized with the injection (detection) efficiency of 100%.
[9] S. Datta, in *Electronic Transport in Mesoscopic Systems* (Cambridge University Press, Cambridge, 1995).
[10] J. Luo *et al.*, Phys. Rev. B **41**, 7685 (1990).
[11] J. P. Heida *et al.*, Phys. Rev. B **57**, 11911 (1998).
[12] M. Schultz *et al.*, Semicond. Sci. Technol. **11**, 1168 (1996); J. Hong *et al.*, J. Korean Phys. Soc. **45**, 197 (2004).
[13] T. Matsuyama *et al.*, Phys. Rev. B **65**, 155322 (2002); F. Mireles and G. Kirczenow, Phys. Rev. B **66**, 214415 (2002).
[14] See for instance Eq. (1) in T. P. Pareek and P. Bruno, Phys. Rev. B **65**, 241305(R) (2002).
[15] To mimic ideal injector and collector, the tunneling matrix elements for tunneling of unfavored spin into the injector (collector) have been set to zero and the parameters for the injector (collector) are chosen to minimize the mismatch between the injector (collector) and the 2DEG.
[16] R. J. Elliot, Phys. Rev. **96**, 266 (1954); Y. Yafet, in *Solid State Physics*, Vol. 14, edited by F. Seitz and D. Turnbull (Academic, New York).
[17] W. Häusler, Phys. Rev. B **63**, 121310 (2001).
[18] A. V. Moroz and C. H. W. Barnes, Phys. Rev. B **60**, 14272 (1999); M. Governale and U. Zülicke, Phys. Rev. B **66**, 073311 (2002).
[19] The α-dependence of the scattering amplitudes can be essentially ignored as long as $\hbar v_F \gg \alpha$ and l/L is not extremely small.
[20] Y. Gefen *et al.*, Phys. Rev. Lett. **52**, 129 (1984).
[21] P. A. Lee and A. D. Stone, Phys. Rev. Lett. **55**, 1622 (1985).
[22] A. I. Larkin and D. E. Khmel'nitskii, Zh. Eksp. Teor. Fiz. **91**, 1815 (1986) [Sov. Phys. JETP **64**, 1075 (1986)].
[23] A. L. Yeyati and M. Büttiker, Phys. Rev. B **52**, R14360 (1995).
[24] Equation (5) in Ref. 20 contains a term ($\beta' \sin\phi$) that is not consistent with the phase locking in Ref. 23. A careful examination shows however that the coefficient β' vanishes identically.
[25] A. D. Stone and Y. Imry, Phys. Rev. Lett. **56**, 189 (1986).
[26] For $l/L \ll 1$, the phenomenon of the strong localization (Ref. 9) occurs and $G \sim (e^2/h)\exp(-2L/l)$.